Role of weak zone orientation in continental lithosphere extension

J. W. van Wijk

Scripps Institution of Oceanography, La Jolla, California, USA

Received 8 December 2004; accepted 5 January 2005; published 26 January 2005.

[1] Lithosphere extension and continental breakup axes are often (sub-) parallel to orogenic belts and suture zones. In an attempt to understand the relation between weak zone orientation and extension direction, a 3-D numerical model is developed with which the following aspects are studied: the relation between weak zone axis and axis of maximum crustal deformation, the amount and distribution of crustal thinning, and subsequent implications for rift (a)symmetry. The results suggest that upon oblique extension, rifts develop within the weak zone that individually cross the inherited structure, while as a group they follow the weak trend. This results in an alternating rift asymmetry; the pattern of crustal thinning, topography and thermal structure are not symmetric around the rift axes of the major rift zones and change along-axis over such a rift. This is a possible explanation for alternating asymmetric rift structures such as observed in the East African Rift system. **Citation:** van Wijk, J. W. (2005), Role of weak zone orientation in continental lithosphere extension, *Geophys. Res. Lett.*, *32*, L02303, doi:10.1029/2004GL022192.

1. Introduction

[2] Inherited structures in continental lithosphere play an important role in controlling the location of extension and continental breakup, and the rift evolution. Extension of continental lithosphere is found to follow preferentially pre-existing weak zones like young orogenic belts and suture zones, while stronger cratonic regions are usually not significantly deformed. An orogenic zone where the crust has been tectonically thickened forms a preferred location for lithosphere extension; gravitational collapse of the thickened crust in constructive combination with far-field plate boundary forces is thought to be a main cause of intra-plate extension [*Ziegler and Cloetingh*, 2004]. In an alternative explanation, *Vauchez et al.* [1997, 1998] argue that mechanical anisotropy of the lithospheric mantle below collisional belts causes continental rifting parallel to these structures.

[3] Examples of this tendency are widespread, and include the East African Rift system, rifting between Norway and East Greenland that is probably concentrated along the trend of the Caledonian orogeny, rifting between North America and West Africa following the Appalachian and Mauritanide orogenic trends, and the Rio Grande rift along the axis of Laramide uplift in western North America. Two-dimensional numerical simulations show that pre-existing structures in the lithosphere may determine the thermal structure and thus timing and extent of volcanism during rifting, uplift and subsidence patterns, duration of rifting, and geometry of the resulting margins [e.g., *Dunbar and Sawyer*, 1989a; *Buck*, 1991; *Tommasi and Vauchez*, 2001; *Corti et al.*, 2003]. Not only the nature and extent of a lithosphere weakness are suggested to influence the rifting process, but also the orientation of the pre-existing structure is thought to be important. Patterns of subsidence indicate that the orientation of the pre-existing structural grain relative to the break-up axis may contribute to the amount of continental extension prior to breakup [*Dunbar and Sawyer*, 1989b]. Passive margins of the Central and North Atlantic Oceans show a trend where continental breakup involves significantly less pre-breakup extension where it follows the inherited structural orientation than where it crosses the inherited orientation. Also, observed conjugate margin asymmetry is suggested to result from the orientation of the weak structure with respect to the breakup axis [*Dunbar and Sawyer*, 1989b]. Laboratory experiments in which oblique extension of the rift trend is examined [e.g., *Bonini et al.*, 1997] show that the pattern of faulting during continental rifting is influenced by the orientation of the pre-existing structure.

[4] In an attempt to gain qualitative understanding of the relation between inherited weak structure orientation and the orientation of far field extensional forces during continental rifting, lithosphere extension is simulated with a thermal-mechanical numerical model. In a three-dimensional tectonic setting the following aspects of the process are handled: the relation between weak trend axis and axis of maximum crustal deformation, the amount and distribution of crustal thinning, and subsequent implications for rift (a)symmetry. Initial results presented in the following sections indicate that the relative orientations of weak structure and far field forces influence the rifting process.

2. Models of Continental Lithosphere Extension

[5] 3-D Analogue models have been applied successfully to study extensional tectonics [*Rahe et al.*, 1998; *Basile and Brun*, 1999; *Chemenda et al.*, 2002] and the fault patterns resulting from oblique rifting [*Withjack and Jamison*, 1986; *Tron and Brun*, 1991; *Bonini et al.*, 1997]. Analogue modeling studies necessarily invoke important simplifications such as the (temperature dependent) lithosphere rheology, which is where benefits of numerical models are expected compared to analogue models. In this study a numerical approach is used to simulate extensional deformation of continental lithosphere. The mechanical part of the 3-D finite element code is based on Tecton [*Melosh and Raefsky*, 1980]. It has been modified to be fully three-dimensional, allow for temperature-dependent power law rheology and buoyancy forces, and it includes a correction for brittle/ductile behavior. Visco-elastic deformation in the lithosphere is described in the numerical simulations by a

0094-8276/05/2004GL022192$05.00

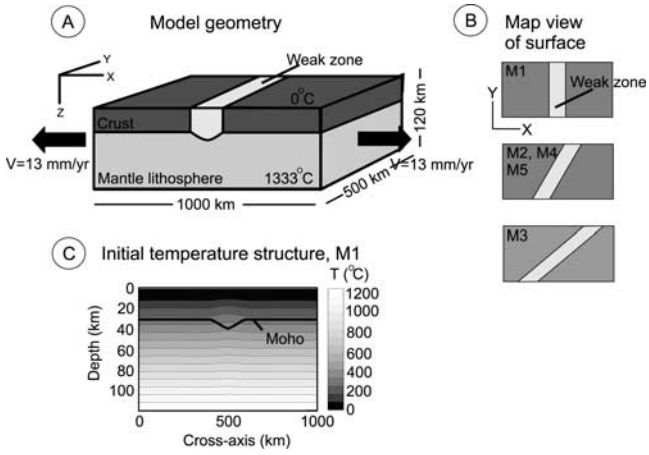

Figure 1. Modeling setup. (a) Configuration and boundary conditions. A weak zone (light gray color) is introduced by locally thickening the crust. Lithosphere is extended by applying constant plate velocity boundary conditions on the left and right sides of the domain. Except for test M4, where the total extension velocity is 15 mm/yr, total extension velocity is constant (26 mm/yr). Crustal thickness is 32 km, and thickened to 40 km in tests M1 to M4 as indicated. In test M5 the crust is thickened from 32 km to 36 km in the weak zone. (b) Orientation of weak trends for tested models M1 to M5 discussed in the text, map view of model domain in Figure 1a. Orientation varies between most favorable (top panel) to least favorable (bottom panel). Weak trend orientations for tests M4 and M5 are the same as for test M2. (c) Profile of the temperature results indicating the initial thermal structure.

Maxwell body. To represent the rheology of the lithosphere at low temperatures and stresses, where it approximates brittle deformation, it is assumed that rocks are fractured extensively, and strength is controlled by friction along preexisting faults, and Byerlee's law is adopted [*Byerlee*, 1987; *Brace and Kohlstedt*, 1980; *Fletcher and Hallet*, 1983]. At high stresses, the value of the yield stress is given by the power law breakdown stress [*Tsenn and Carter*, 1987]. In the simulations density follows a linear equation of state and only thermal buoyancy is considered. Thermal expansion is believed to be the largest source of density gradients in the mantle beneath rifts.

[6] The mechanical part is coupled to a thermal finite element routine based on *Greenough and Robinson* [2000], where the heat flow equation is solved every time step on the same grid as the displacement field. Heat production in the crust is taken to be constant in the simulations. The Lagrangian approach is used, which means that material is attached to the nodes. Advection of heat is accounted for by the nodal displacements, and the mechanical and thermal parts are furthermore coupled through temperature dependent power law rheology and the equation of state.

[7] The equations are solved using the finite element method. The model domain is 1000 × 500 × 120 km (x × y × z). The mesh contains 9375 nodal points and is non-equidistant, finest near the zone of crustal weakness in the x-direction (node spacing about 8 km), and in the crustal layers (node spacing 3 km). These initial numerical tests allow us to address overall behavior of the model, focusing on results that are found to be robust despite the somewhat coarse node spacing.

[8] Simulations are started with an equilibrium thermal state. A constant temperature is adopted for the surface and base of the domain (respectively 0°C and 1333°C). Through the sides of the model a zero heat flow boundary condition is prescribed. Plate velocity boundary conditions for the mechanical model are applied parallel to the x-direction on the left and right sides (Figure 1). The back and front sides are kept fixed in the y-direction and free to move in x- and z-directions. The base of the model is held horizontal but free to move in the x- and y-directions and the top surface is free to deform. The rheological and thermal values used in the different tests are given in Table 1. The lithosphere is rheologically layered and consists of crust and mantle lithosphere portions (Table 1). The crust consists of an upper crust and lower crust of equal thickness and rheology, but different densities. Crustal rheology is based on a quartz diorite composition, for the mantle part of the domain an olivine composition is adopted.

[9] Inherited orogenic structures are represented in the models by weak trends with different orientation with respect to the sides of the model domain where plate velocity boundary conditions are prescribed. The zone where crustal thickness is increased from its standard thickness of 32 km to a thickness of 40 km defines the weak zone (Figure 1); the tectonically thickened crust is introduced in the model as an elongated area where the crust has been thickened in the initial setup. In this way, stronger mantle material is replaced by weaker crust material, and this creates a weak trend in the lithosphere. This is one simplified representation of a weak trend; other suggested sources of weakness in the lithosphere not necessarily reproduced here are rheological heterogeneity [*Dunbar and Sawyer*, 1989a], mechanical anisotropy of the mantle [*Vauchez et al.*, 1997, 1998], thermal disturbance such as hot spots [*Hill*, 1991] or base-lithosphere pre-existing topography [*Ebinger and Sleep*, 1998; *Pascal et al.*, 2002]. Two-dimensional finite element simulations have indicated that the nature of the weak zone affects the strain localization process; however, this is outside the scope of the present study. The width of the weak zone is 200 km from one side to the other, with significant crustal thickening (>4 km) in a 100 km wide zone.

Table 1. Material Parameter Values From *Turcotte and Schubert* [2002] and *Kirby and Kronenberg* [1987][a]

	Upper Crust	Lower Crust	Mantle
Rheological parameters			
Density	2700	2800	3300
Young's modulus	$5 \cdot 10^{10}$	$5 \cdot 10^{10}$	$1 \cdot 10^{10}$
Poisson's ratio	0.25	0.25	0.25
Power law exponent n	3.0	3.0	3.0
Activation energy Q	219	219	555
Material constant A	$5.0 \cdot 10^{-18}$	$5.0 \cdot 10^{-18}$	$7.0 \cdot 10^{-14}$
Thermal parameters			
Conductivity	2.4	2.4	3.0
Specific heat	1050	1050	1050
Thermal expansion	$1 \cdot 10^{-5}$	$1 \cdot 10^{-5}$	$1 \cdot 10^{-5}$
Heat production	$1 \cdot 10^{-6}$	$1 \cdot 10^{-6}$	-

[a]Crust: quartz diorite composition, mantle part: olivine composition. Density [kgm^{-3}], Young's modulus [Pa], activation energy [$kJmole^{-1}$], material constant [$Pa^{-n}s^{-1}$], conductivity [$Wm^{-1}K^{-1}$], specific heat [$Jkg^{-1}K^{-1}$], thermal expansion [K^{-1}], heat production [Wm^{-3}].

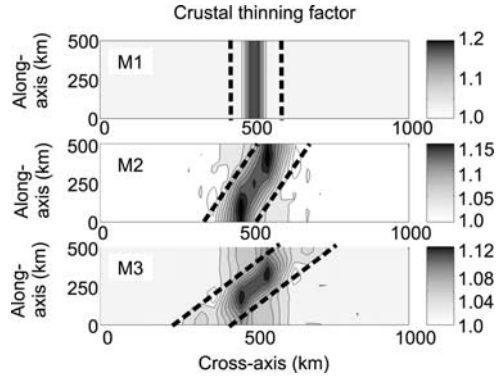

Figure 2. Modeling results. Crustal thinning factors in map view for three different orientations of the weak trend (Figure 1b) after 4 My of model evolution. Boundaries of the weak trend are super-positioned (white dashed lines). Individual rifts cross the weak trend, as a group they follow the weak trend. See color version of this figure in the HTML.

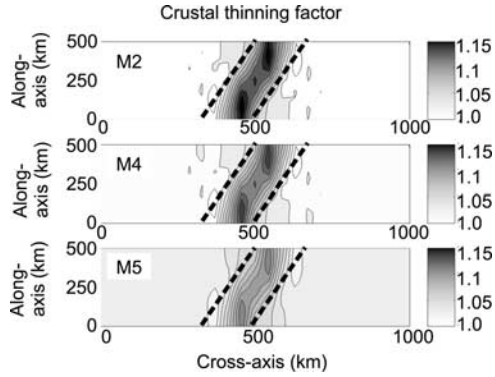

Figure 3. Modeling results after 4 My. Crustal thinning factors for tests M2 (upper panel), with extension velocity of 26 mm/yr and initial Moho depression 40 km, M4 and M5 (lower panel). In test M4 the total extension velocity is 15 mm/yr, in test M5 the prescribed initial weak zone crustal thickness is 36 km. See color version of this figure in the HTML.

[10] The lithosphere is not extended to the point that the breakup process and passive margin formation are represented; in the initial simulations presented below, numerical experiments are run for about 4 to 5 My. With longer runs we find the grid to be seriously distorted, and this could affect the accuracy of the results. These initial runs provide useful information and they avoid remeshing, which will be required for longer runs. The model geometry and orientations of the weak zone in the different tests are shown in Figure 1.

3. Results

[11] Below we present results of five different tests, M1 to M5, in which the orientation of the weak trend, the crustal thickness, and the amplitude of the plate boundary velocity are varied. Test M1 is the standard test in which the weak trend axis is favorably oriented parallel to the right and left sides of the domain. In tests M2 and M3 the angle between the weak trend axis and the right and left sides is varied. The orientation of the weak trend is the same in test M4 as in test M2, but the amplitude of the extension velocity is decreased to 15 mm/yr in test M4. In test M5 the weak trend has the same orientation as in test M2, but the crust is less thickened in the weak zone; to 36 km instead of 40 km.

[12] Upon extension of the lithosphere, deformation localizes more or less strongly in the weak zone, dependent on the model tested. The crust is thinned and warm mantle material wells up below the rift axis (Figures 1 and 2). In the favorably oriented weak zone test M1, the rift develops symmetrically, with largest crustal thinning factors in the 100 km wide center of the zone. Away from the central zone crustal thinning is predicted to decrease rapidly. This basically two-dimensional result is in line with prior 2-D finite element simulations that predict localized deformation in a small zone when the width of the weak trend is small [*Corti et al.*, 2003]. The major rift zones still follow the weak trend location as a group in test M2, but are individually oriented according to the extension direction; i.e., rotated with respect to the weak trend. Maximum crustal thinning factors (defined as the ratio between the initial crust thickness and its thickness after 4 My of model evolution) are less, and the rift zone is wider. This is even more the case for test M3; the thinning pattern is asymmetric and wide. Again, individual rift zones cross the weak trend but follow the trend as a group.

[13] In tests M4 and M5 the extension velocity and, respectively, crustal thickness are varied with respect to test M2. The main effect of a different extension velocity on thinning factors is that amplitudes between modeling results are different (Figure 3). Changing the weak zone crustal thickness results in a somewhat different distribution of crustal thinning in test M5, deformation is less localized and rifting is predicted to occur over a wider area. The distribution of crustal thinning reflects the asymmetric deformation in the lithosphere in simulations where the axes of inherited structures are oblique with respect to the

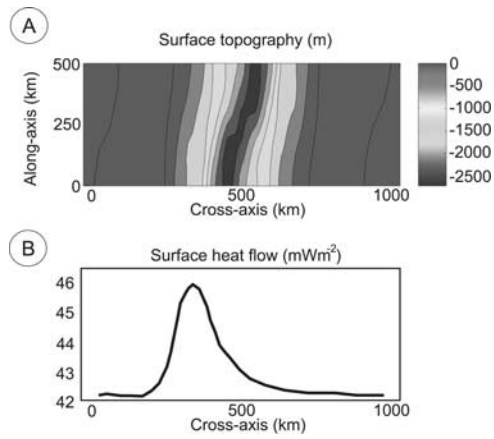

Figure 4. (a) Surface topography test M2, map view, (b) surface heat flow for test M3, at y = 125 km. Surface heat flow calculated using $q = -k\partial T/\partial z$, where q is the surface heat flow and k is conductivity. Because surface processes (erosion, sedimentation) are not included in the model, topography should be considered a first-order result only. See color version of this figure in the HTML.

extension. Resulting surface topography (Figure 4a) and thermal structure, reflected in the surface heat flow (Figure 4b), are predicted to be asymmetric as well, and this asymmetry changes along the rift axes. Rifts are thus expected to develop with alternating asymmetry. We find that areas where crustal thinning occurs develop in the first 4 My of extension, and then do not change during further model evolution. Performed model runs only simulate continental extension during a 4 to 5 My long period, however there are no indications that the rifts shift or rotate in time, only thinning factor amplitudes change with ongoing lithosphere extension.

[14] Analogue modeling studies that have conducted similar experiments also predict asymmetrical rift geometry upon oblique extension [*Withjack and Jamison*, 1986; *Tron and Brun*, 1991; *Bonini et al.*, 1997]. Numerical results that are in line with analogue predictions include furthermore extensional deformation that is less when extension is more oblique and a deformed zone that is rotated with respect to the weak trend to become more parallel to the extension. A difference is that the deforming zone becomes narrower upon oblique extension in analogue experiments while it becomes wider in the numerical experiments.

4. Rift Asymmetry: The East African Rift System

[15] The East African Cenozoic rifts have developed mainly within Proterozoic belts. On a continental scale this relation is obvious, while on the local scale of individual rift basins or faults the relation with pre-existing structures is more complicated. Alternating asymmetric rift structures linked through accommodation zones characterize some parts of the East African rift [*Bosworth*, 1987; *Ebinger et al.*, 1987]. This observation has been interpreted in several ways, including a simple shear model [*Bosworth*, 1987], rift propagation, and mantle diapiric upwelling [*Ebinger et al.*, 1987].

[16] The modeling results offer a possible alternative explanation for this observation. The results suggest that upon oblique rifting, the major rift zones (where the largest crustal thinning factors are predicted) individually cross the inherited structure (Figures 2 and 3). This results in an alternating rift asymmetry; the pattern of crustal thinning, topography and thermal structure are not symmetric around the rift axes of the major rift zones and change along-axis over such a rift. It is beyond current simulation possibilities to predict fault patterns and locations of accommodation zones with the model, but it is possible that these asymmetric conditions may result in alternating asymmetry trends as observed at some continental rifts. Observed spacing between the central parts of adjoining alternating asymmetric rifts is ~70 km [*Ebinger et al.*, 1987] in the Malawi Rift. Although the initial modeling results suggest a spacing of the same order, more experiments are needed to investigate the preferred length scale and controlling parameters.

[17] **Acknowledgments.** Donna Blackman and Neal Driscoll are thanked for stimulating discussions and suggestions on this manuscript. Jacques Deverchere and an anonymous reviewer are thanked for detailed and constructive comments. This work is supported by National Science Foundation grant EAR-0105896.

References

Basile, C., and J. P. Brun (1999), Transtensional faulting patterns ranging from pull-apart basins to transform continental margins: An experimental investigation, *J. Struct. Geol.*, *21*, 23–37.

Bonini, M., T. Souriot, M. Boccaletti, and J. P. Brun (1997), Successive orthogonal and oblique extension episodes in a rift zone: Laboratory experiments with application to the Ethiopian rift, *Tectonics*, *16*, 347–362.

Bosworth, W. (1987), Off-axis volcanism in the Gregory rift, east Africa: Implications for models of continental rifting, *Geology*, *15*, 397–400.

Brace, W. F., and D. L. Kohlstedt (1980), Limits on lithospheric stress imposed by laboratory experiments, *J. Geophys. Res.*, *85*, 6248–6252.

Buck, W. R. (1991), Modes of continental lithosphere extension, *J. Geophys. Res.*, *96*, 20,161–20,178.

Byerlee, J. (1987), Friction of rocks, *Pure Appl. Geophys.*, *116*, 615–626.

Chemenda, A., J. Déverchère, and E. Calais (2002), Three-dimensional laboratory modeling of rifting: Application to the Baikal rift, Russia, *Tectonophysics*, *356*, 253–273.

Corti, G., J. Van Wijk, M. Bonini, D. Sokoutis, S. Cloetingh, F. Innocenti, and P. Manetti (2003), Transition from continental break-up to punctiform seafloor spreading: How fast, symmetric and magmatic, *Geophys. Res. Lett.*, *30*(12), 1604, doi:10.1029/2003GL017374.

Dunbar, J. A., and D. S. Sawyer (1989a), How pre-existing weaknesses control the style of continental breakup, *J. Geophys. Res.*, *94*, 7278–7292.

Dunbar, J. A., and D. S. Sawyer (1989b), Patterns of continental extension along the conjugate margins of the central and north Atlantic Oceans and Labrador Sea, *Tectonics*, *8*, 1059–1077.

Ebinger, C. J., and N. H. Sleep (1998), Cenozoic magmatism throughout east Africa resulting from impact of a single plume, *Nature*, *395*, 788–791.

Ebinger, C. J., B. R. Rosendahl, and D. J. Reynolds (1987), Tectonic model of the Malawi rift, Africa, *Tectonophysics*, *141*, 215–235.

Fletcher, R. C., and B. Hallet (1983), Unstable extension of the lithosphere: A mechanical model for basin and range structure, *J. Geophys. Res.*, *88*, 7457–7466.

Greenough, C., and K. R. Robinson (2000), FELIB: The Finite Element Library, release 4.0, Math. Software Group, Rutherford Appleton Lab., Chilton, U. K., available at http://www.mathsoft.cse.clrc.ac.uk.

Hill, R. I. (1991), Starting plumes and continental break-up, *Earth Planet. Sci. Lett.*, *104*, 398–416.

Kirby, S. H., and A. K. Kronenberg (1987), Rheology of the lithosphere: Selected topics, *Rev. Geophys.*, *25*, 1219–1244.

Melosh, H. J., and A. Raefsky (1980), The dynamical origin of subduction zone topography, *Geophys. J. R. Astron. Soc.*, *60*, 333–354.

Pascal, C., J. W. van Wijk, S. A. P. L. Cloetingh, and G. R. Davies (2002), Effect of lithosphere thickness heterogeneities in controlling rift localization: Numerical modeling of the Oslo Graben, *Geophys. Res. Lett.*, *29*(9), 1355, doi:10.1029/2001GL014354.

Rahe, B., D. A. Ferrill, and A. P. Morris (1998), Physical analog modeling of pull-apart basin evolution, *Tectonophysics*, *285*, 21–40.

Tommasi, A., and A. Vauchez (2001), Continental rifting parallel to ancient collisional belts: An effect of the mechanical anisotropy of the lithospheric mantle, *Earth Planet. Sci. Lett.*, *185*, 199–210.

Tron, V., and J. P. Brun (1991), Experiments on oblique rifting in brittle-ductile systems, *Tectonophysics*, *188*, 71–84.

Tsenn, M. C., and N. L. Carter (1987), Upper limits of power law creep of rocks, *Tectonophysics*, *136*, 1–26.

Turcotte, D. L., and G. Schubert (2002), *Geodynamics*, 2nd ed., 456 pp., Cambridge Univ. Press, New York.

Vauchez, A., G. Barruol, and A. Tommas (1997), Why do continents break-up parallel to ancient orogenic belts?, *Terra Nova*, *9*, 62–66.

Vauchez, A., A. Tommasi, and G. Barrruol (1998), Rheological heterogeneity, mechanical anisotropy and deformation of the continental lithosphere, *Tectonophysics*, *296*, 61–86.

Withjack, M. O., and W. R. Jamison (1986), Deformation produced by oblique rifting, *Tectonophysics*, *126*, 99–124.

Ziegler, P. A., and S. A. P. L. Cloetingh (2004), Dynamic processes controlling evolution of rifted basins, *Earth Sci. Rev.*, *64*, 1–50.

J. W. van Wijk, Scripps Institution of Oceanography, La Jolla, CA 92093-0225, USA. (jvanwijk@ucsd.edu)